0021-972X/04/$15.00/0
Printed in U.S.A.

The Journal of Clinical Endocrinology & Metabolism 89(8):4104–4112

doi: 10.1210/jc.2003-031432

Localization of Osteoprotegerin, Tumor Necrosis Factor-Related Apoptosis-Inducing Ligand, and Receptor Activator of Nuclear Factor-κB Ligand in Mönckeberg's Sclerosis and Atherosclerosis

MICHAEL SCHOPPET, NADIA AL-FAKHRI, FOLKER E. FRANKE, NORBERT KATZ, PETER J. BARTH, BERNHARD MAISCH, KLAUS T. PREISSNER, AND LORENZ C. HOFBAUER

Departments of Internal Medicine and Cardiology (M.S., B.M.), Gastroenterology, Endocrinology and Metabolism (L.C.H.), and Pathology (P.J.B.), Philipps University, D-35033 Marburg, Germany; and Departments of Clinical Chemistry (N.A.-F., N.K.), Pathology (F.E.F.), and Biochemistry (K.T.P.), Justus Liebig University, D-35390 Giessen, Germany

Vascular calcification may occur at different areas of the vessel wall, including the intima in atherosclerosis and the media in Mönckeberg's sclerosis. Medial calcification of arteries is common in patients with diabetes mellitus or chronic renal failure. Osteoprotegerin (OPG) and receptor activator of nuclear factor-κB ligand are essential modulators of bone homeostasis and may be involved in the process of vascular calcification. In this study we investigated arteries from patients with Mönckeberg's sclerosis and atherosclerosis. Apoptosis, which precedes vascular calcification *in vitro*, was assessed by an *in situ* ligation assay and was localized to the medial layer of arteries (Mönckeberg's sclerosis) and the neointima (atherosclerosis). Immunohistochemistry and *in situ* hybridization revealed OPG immunoreactivity and mRNA expression surrounding calcified areas in the medial layer (Mönckeberg's sclerosis), whereas OPG was mainly expressed adjacent to calcified neointimal lesions (atherosclerosis). Receptor activator of nuclear factor-κB ligand protein and mRNA were barely or not detectable. Of note, TNF-related apoptosis-inducing ligand, an inducer of apoptosis that is also blocked by OPG, displayed a similar spatial distribution as OPG. In summary, we demonstrate enhanced apoptosis adjacent to vascular calcification, and the concurrent expression of regulators of apoptosis and osteoclastic differentiation, TNF-related apoptosis-inducing ligand and OPG, suggesting their involvement in the pathogenesis of vascular calcification. (*J Clin Endocrinol Metab* 89: 4104–4112, 2004)

VASCULAR CALCIFICATION IS considered to be a component of vascular disease distinct from atheroma formation, and apoptosis has been shown to be an initiator of mineralization in recent *in vitro* studies (1). Heterotopic vascular calcification of the medial vessel wall layer in Mönckeberg's sclerosis occurs independently and at a distinct site compared with atherosclerotic lesions. In contrast to Mönckeberg's sclerosis, intimal calcification in atherosclerosis is associated with hyperlipidemia, macrophage recruitment, and inflammation (2). Mönckeberg's sclerosis progresses with age and is common in patients with diabetes mellitus and chronic renal failure. Of note, Mönckeberg's sclerosis is strongly associated with metabolic bone disease, such as osteoporosis (3). Both intimal and medial calcification are associated with significant morbidity and mortality (4).

Osteoprotegerin (OPG) and receptor activator of nuclear factor-κB (RANK) ligand (RANKL) are novel members of the TNF ligand and receptor signaling family, respectively, that constitute the final effectors of osteoclast function and therefore represent essential regulators of bone mass and bone homeostasis (5). RANKL is expressed by osteoblastic lineage cells and T lymphocytes and acts by binding to its physiological receptor, RANK, which is expressed on osteoclasts (6). Ligation of the receptor stimulates all aspects of osteoclast function, such as differentiation, maturation, fusion, survival, and activity. By contrast, OPG is produced by a variety of tissues, including the cardiovascular system, and acts as a soluble decoy receptor by neutralizing RANKL. OPG also represents a receptor for the cytotoxic ligand TNF-related apoptosis-inducing ligand (TRAIL) (7), a potent activator of apoptosis after binding to death domain homolog-containing receptors (8).

OPG-deficient mice exhibit a phenotype of osteoporosis, and two thirds of the animals also display medial calcifications of the aorta and the renal arteries (9) that can be successfully treated by an OPG transgene delivered during midgestation (10). In addition, RANKL and RANK transcripts could be demonstrated in calcified arterial lesions of OPG-deficient mice, but not wild-type mice (10). We hypothesized that regulators of bone metabolism, such as OPG and RANKL, may be expressed in the vicinity of calcified regions in Mönckeberg's sclerosis and atherosclerosis, and that apoptosis may be involved in the process of calcification.

Abbreviations: DIG, Digoxigenin; DNase, deoxyribonuclease; EC, endothelial cells; ISL, *in situ* ligation assay; NBT/BCIP, nitro blue tetrazolium/5-bromo-4-chloro-3-indolyl-phosphate; OPG, osteoprotegerin; RANK, receptor activator of nuclear factor-κB; RANKL, RANK ligand; RNase, ribonuclease; SSC, sodium citrate buffer; TRAIL, TNF-related apoptosis-inducing ligand; VSMC, vascular smooth muscle cells.

JCEM is published monthly by The Endocrine Society (http://www.endo-society.org), the foremost professional society serving the endocrine community.

Patients and Methods

Patient samples

Mönckeberg's medial sclerosis was diagnosed according to defined histological criteria (11, 12), including widespread medial calcifications and partially ossification. Specimens were termed atherosclerotic if only neointimal lesions were found; these specimens showed advanced atherosclerotic lesion types and calcifications in the neointima (types IV–VIa) (13). All specimens were examined by two experienced investigators. Specimens of Mönckeberg's sclerosis were obtained from six patients immediately after lower limb amputation or at autopsy. Four of these specimens had only medial calcifications and minor or no intimal thickening; two specimens had medial and neointimal calcifications. Atherosclerotic tissues were obtained from two carotid artery specimens collected during carotid eversion endarterectomy of patients with carotid stenosis and from four femoral and iliac artery specimens collected during lower limb bypass surgery from patients with femoral artery stenosis. Two control specimens were obtained from normal femoral arteries, two controls derived from normal internal mammary arteries. Control arteries showed no histopathological signs of neointima development or medial sclerosis. The study was approved by the institutional review board of Justus Liebig University Giessen. The tissue samples used were waste material that would have otherwise been discarded after the surgical procedure.

Tissue embedding, processing, and conventional staining

All specimens were fixed for 12 h with 4% formaldehyde/PBS from 2–5 h after surgical excision or at autopsy 8–12 h postmortem and then paraffin-embedded. Specimens were cut in serial sections of 6 μm without prior decalcification to avoid denaturation of protein or RNA (14). Tissue integrity was demonstrated by hematoxylin and eosin staining of specimens. Sections were mounted on slides coated with aminopropyltriethoxysilane (Sigma-Aldrich Corp., Taufkirchen, Germany). After deparaffinization and rehydration, serial sections of all specimens were subjected to *in situ* ligation assay (ISL), immunohistochemistry, and *in situ* hybridization. Additional serial sections of all specimens were subjected to von Kossa staining and kernechtrot (4-amino-9,10-dihydro-1,3-dihydroxy-9,10-dioxo-2-anthracen sulfonate) counterstaining to demonstrate calcifications as well as to conventional hematoxylin and eosin staining for histopathological analysis. Five sites per specimen, 50 μm distance from each other, were investigated; all analyses were repeated four to six times. All specimens were analyzed by two experienced investigators by assessing semiquantitatively the average staining intensity and the typical staining pattern of the whole section circumference.

ISL

The ISL (or T4 DNA ligation assay) (15) was employed as described previously (16). It demonstrates the apoptosis-specific form of DNA fragmentation, *i.e.* 3′ single base overhang, double-stranded DNA breaks. Briefly, a 3′ single base overhang DNA probe was prepared by PCR using primers 5′-TCACTAAAGGGAACAAAAGC-3′ and 5′-ACTATAGGGCGAATTGGAG-3′, complementary to the T3 and T7 promoters in the multicloning site of plasmid Bluescript II $KS^{+/-}$ (Stratagene, La Jolla, CA). The PCR product was separated by electrophoresis on 2% agarose gels (Pharmacia Biotech, Erlangen, Germany) in Tris-acetate-EDTA buffer, stained with ethidium bromide, excised from the gel, and purified with the Qiaex II gel extraction kit (Qiagen, Hilden, Germany).

After deparaffinization and rehydration, slides were treated with proteinase K (20 μg/ml) for 10 min and postfixed in 4% methanol-free formaldehyde/PBS. For the positive control, a specimen was preincubated with Tris buffer (pH 7.9) containing 1 μg/ml deoxyribonuclease I (DNase I) for 10 min and processed separately thereafter. All slides were then incubated with a mixture of 50 mM Tris-HCl (pH 7.8), 10 mM $MgCl_2$, 10 mM dithiothreitol, 1 mM ATP, 25 μg/ml BSA, 15% polyethylene glycol, 3 μg/ml digoxigenin (DIG)-labeled DNA fragment, and 32 U/ml DNA T4 ligase (Sigma-Aldrich Corp.) in a humidified chamber for 1 h at room temperature. For the negative control, either the DIG-labeled DNA fragment or DNA T4 ligase was omitted in the incubation mixture. The slides were then washed in 60 C deionized water. Slides were preblocked with normal sheep serum and incubated with sheep anti-DIG Fab antibody conjugated to alkaline phosphatase (Roche, Mannheim, Germany; 1:500) for 30 min. Color development was performed with nitro blue tetrazolium/5-bromo-4-chloro-3-indolyl-phosphate [NBT/BCIP; 100 mM Tris (pH 9.5), 100 mM NaCl, 50 mM $MgCl_2$, 0.38 mg/ml NBT, 0.18 mg/ml BCIP, and 1 mM levamisole (Sigma-Aldrich Corp.)] for 70 min at room temperature. The reaction was terminated by deionized water, ISL and conventionally stained serial sections were examined for the scoring of cells undergoing apoptosis by light microscopy at 400-fold magnification. The apoptotic index was determined by counting the number of ISL-positive nuclei on a total of 500 cell nuclei/slide and calculating the mean as a percentage of all slides.

Immunohistochemistry

Slides were preincubated with 5% normal goat or rabbit serum, then incubated with antibodies against OPG (two antihuman OPG mouse monoclonal antibodies, clones 69146.11 and 69127.11; R&D Systems, Minneapolis, MN; 12.5 μg/ml), RANKL (antihuman RANKL mouse monoclonal antibody, clone 70525.11; R&D Systems; 25 μg/ml), TRAIL (antihuman TRAIL goat polyclonal antibody, K-18; Santa Cruz Biotechnology, Santa Cruz, CA; 10 μg/ml; and antihuman TRAIL mouse monoclonal antibody, clone 75411.11, R&D Systems; 50 μg/ml), human smooth muscle α-actin (mouse monoclonal antibody, clone 1A4; Dakocytomation, Hamburg, Germany; 1.5 μg/ml), human macrophage antigen CD68 (mouse monoclonal antibody, clone KP1; Dakocytomation; 4.3 μg/ml), human T lymphocyte antigen CD3 (mouse monoclonal antibody, clone T3-4B5; Dakocytomation; 2.3 μg/ml), and human B lymphocyte antigen CD21 (mouse monoclonal antibody, clone 1F8; Dakocytomation; 3.5 μg/ml). Negative controls were conducted by substituting the specific primary antibody with an irrelevant antibody. Subsequently, specimens were incubated with biotinylated goat anti-mouse antibody (Sigma-Aldrich Corp.) or biotinylated rabbit antigoat antibody (Dakocytomation), streptavidin-alkaline phosphatase-conjugate, Fast Red stain (all reagents from Sigma-Aldrich Corp.), and Mayer's hemalum counterstaining. Slides were covered with glycerol-gelatin and coverslips and finally examined by light microscopy.

RNA preparation, RT, and cDNA synthesis

Total cellular RNA was extracted using a modified single step isolation protocol based on established methods (17). For the preparation of RNA to be subjected to cDNA transcription, we employed a vascular smooth muscle cell line for OPG and TRAIL cRNA probes and an osteosarcoma cell line, MG-63, for RANKL cRNA probe (purchased from American Type Culture Collection, Manassas, VA). Cultures of human vascular smooth muscle cells were established from saphenous veins, characterized, and grown exactly as described previously (16). Cells were frozen in liquid nitrogen, homogenized, and lysed in 500 μl TRIzol (Sigma-Aldrich Corp.). RNA concentrations were measured by spectrophotometry and calculated on the basis of OD_{260} values.

Genomic DNA contamination was eliminated by a protocol adapted from previously described methods (18, 19). The solution containing 1 μg/μl RNA was incubated for 30 min at 37 C with 0.09 U/μl ribonuclease (RNase)-free deoxyribonuclease (Promega Corp., Mannheim, Germany), 40 U RNase inhibitors (RNasin, Promega Corp.), and 0.66 mM $MnCl_2$ in 10 mM Tris-HCl (pH 7.8). Before heat inactivation of DNase at 75 C for 5 min, 3 mM EDTA and 0.15 mM dithiothreitol were added to avoid subsequent DNase reactivation (18). Afterward, the reaction mixture was cooled to 42 C. RT was performed at 42 C for 60 min after the addition of 8 U avian myeloblastosis virus reverse transcriptase, 10.55 mM dithiothreitol, 11.34 mM $MgCl_2$, 0.57 μg oligo(deoxythymidine) primer, 0.5 mM deoxy-NTP, and 32 U RNase inhibitors (RT system from Promega Corp.) in a total volume of 21 μl. The reaction was terminated by heat inactivation of reverse transcriptase at 90 C for 5 min. RT products were diluted to 10 ng cDNA/μl in sterile distilled water for subsequent PCR.

The primer pairs (MWG Biotech, Ebersberg, Germany) used for PCR amplification of the cloned sequence that was finally employed for cRNA probe preparation are shown in Table 1. PCR was performed in a final volume of 20 μl containing 20 ng cDNA of a defined specimen, 0.2 mM deoxy-NTP-Mix (Pharmacia Biotech), 0.5 U *Taq* DNA polymerase (Eppendorf, Hamburg, Germany), 10 pmol of each primer, 50 mM

TABLE 1. Primer pairs used in this study

Target	Sense and antisense primers	PCR product size (bp)	GenBank accession no.
OPG	sp n 497-n 517, asp n 760-n 780	284	U94332
RANKL	sp n 557-n 574, asp n 776-n 796	240	AF019047
TRAIL	sp n 282-n 301, asp n 554-n 574	293	U37518

Primer pairs used for PCR synthesis of the cloned cDNA sequence corresponding to the cRNA probe. n, Nucleotide number of the mRNA sequence deposited in the GenBank; sp, sense primer; asp, antisense primer. Intron-flanking primers were derived from the human target mRNA sequence, deposited in GenBank, with the help of Oligo 5.0 software (National Biosciences, Plymouth, MN). This software was also used to check for the absence of false priming sites, the formation of primer dimers, and secondary structures.

KCl in 10 mM Tris-HCl (pH 8.3), and 1.5 mM $MgCl_2$. Individual PCR protocols were employed for every PCR target. PCR products were electrophoresed in 2% agarose gels (Pharmacia Biotech). Specific products were identified after ethidium bromide staining under UV light, excised from the gel, and extracted with Qiaex II agarose gel extraction kit (Qiagen).

cDNA cloning and DIG-labeled cRNA probe preparation

OPG, RANKL, and TRAIL PCR products were subcloned in pGEM-T (Promega Corp.). The plasmids were transformed in the XL1-Blue *Escherichia coli* strain (Stratagene, La Jolla, CA) and extracted by column purification according to the manufacturer's instructions (Qiagen). The concentration and purity of the extracted plasmids were assessed on the basis of OD_{260} values. For cRNA probe synthesis, the vectors containing the insert were digested with *Nco*I or *Not*I (New England Biolabs, Beverly, MA) for the production of sense cRNA (*Nco*I) or antisense cRNA (*Not*I). *In vitro* transcription of DIG-labeled cRNA was performed using the DIG RNA labeling mix and RNA polymerases T7 and SP6 (all reagents from Roche). After precipitation with 8.0 mM LiCl and 100% ethanol extraction, the dried pellet was reconstituted in 100 μl RNase-free water. The concentrations of the DIG cRNA probes were estimated by semiquantitative dot blots.

In situ hybridization

After digestion with 20 μg/ml PBS proteinase K (Promega Corp.) for 25 min at 37 C, sections were incubated in 0.2% glycine and then in 20% acetic acid. The sections were postfixed in 4% paraformaldehyde for 10 min and prehybridized in 20% glycerol for 30 min. Sections were then incubated with the DIG-labeled antisense cRNA probes. All cRNA probes were used at a dilution of 1:100 in hybridization buffer containing 50% deionized formamide, 10% dextran sulfate, 0.3 mM sodium chloride/30 mM sodium citrate (2× SSC buffer), 0.2 mg/ml BSA/0.2 mg/ml Ficoll 400/0.2 mg/ml polyvinylpyrrolidone (Denhardt's solution), 10 μg/ml salmon sperm DNA (Sigma-Aldrich Corp.), and 10 μg/ml yeast tRNA (Sigma-Aldrich Corp.). Hybridization was performed overnight at 37 C in a humidified chamber containing 50% formamide/2× SSC buffer.

Posthybridization washes were preceded by multiple washes in 4× SSC for 15 min at room temperature, slides were then incubated in 4× SSC containing 300 μg/ml RNase A and 10 U/ml RNase T1 (RNase A+T1 mix; BD Pharmingen, San Diego, CA) for 30 min at 37 C. The following washes were carried out: 4× SSC four times for 5 min each time at 37 C, 2× SSC for 15 min at 60 C, 0.2× SSC for 15 min at 42 C, 0.1× SSC for 5 min at room temperature, and 2× SSC for 5 min at room temperature. Slides were preincubated with 5% normal sheep serum and 3% BSA, then incubated overnight at 4 C with a sheep anti-DIG Fab antibody conjugated to alkaline phosphatase (Roche; 1:500). Staining was performed with NBT/BCIP and 1 mM levamisole (Sigma-Aldrich Corp.). Finally, sections were covered with glycerol-gelatin and coverslips. For every hybridization procedure, control incubations of various sections were performed using DIG-labeled cRNA sense probes. In addition, control incubations were performed by substituting the antisense cRNA probes with DIG to rule out unspecific binding.

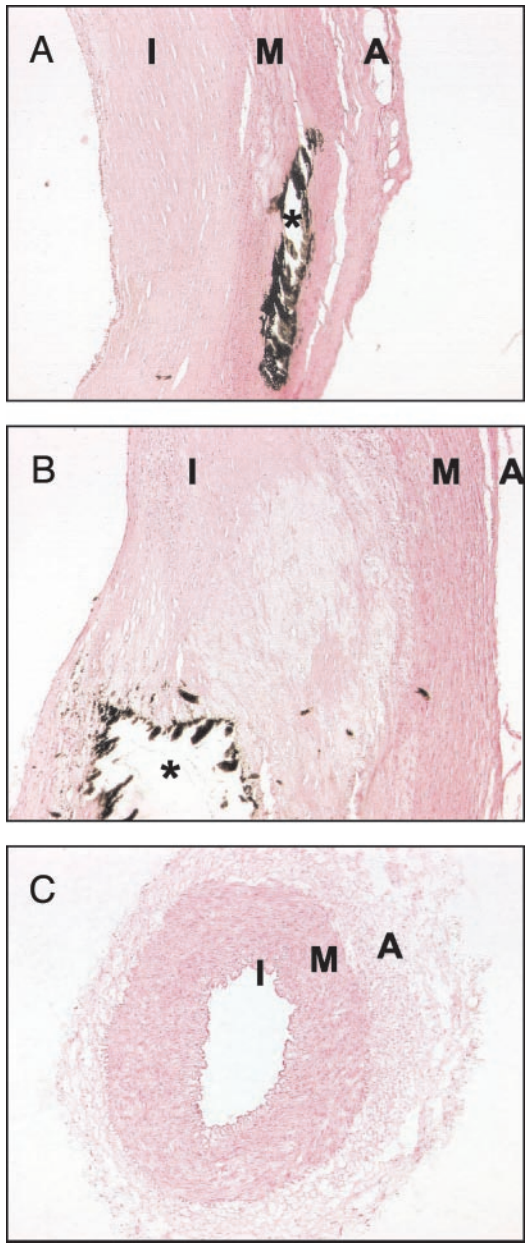

FIG. 1. von Kossa staining of transverse arterial sections demonstrating calcifications (*black* staining) and kernechtrot counterstaining (*red* nuclear staining; all 50-fold magnification). Serial sections of the same specimens as those in A–C are shown in Figs. 2–4. The intimal (I), medial (M), and adventitial (A) layers of the vessels are indicated. A, Proximal femoral artery specimen of a patient with Mönckeberg's sclerosis showing typical medial calcifications (*asterisk*). B, Atherosclerotic artery with large calcification (*asterisk*; calcified material partly detached) and fibroatheromatous lesions in the intima; iliac artery specimen of a patient with a typically enlarged atherosclerotic neointima and an unaffected medial layer. C, Internal mammary artery with normal vascular architecture.

Results

Conventional staining and characterization of lesions

Specimens of normal vessels (n = 4) were compared with Mönckeberg's sclerosis (n = 6) and with atherosclerotic tissue samples (n = 6) by conventional hematoxylin and eosin and von Kossa staining. Calcification was de-

tected in the medial layer in Mönckeberg's sclerosis and in the neointimal layer in atherosclerosis, but not in normal control vessels (Fig. 1). Analysis of vascular lesions by characteristic markers, such as smooth muscle α-actin, macrophage antigen CD68, T lymphocyte antigen CD3, and B lymphocyte antigen CD21, revealed that the medial tissue surrounding calcified lesions in Mönckeberg's sclerosis contained only smooth muscle cells, whereas macrophages and lymphocytes were absent. By contrast, in atherosclerosis, the neointima exhibited foam cell accumulations composed of smooth muscle cells and macrophages, whereas lymphocytes were not detected (data not shown). Analysis of patient data for different variables, such as age, sex, the vascular region investigated, and atherosclerosis risk factors, revealed the well known higher incidence of diabetes and chronic renal failure in patients with Mönckeberg's sclerosis (Table 2A) (4, 12). Comparison of clinical and histological characteristics of atherosclerosis and Mönckeberg's sclerosis patients revealed no association of a single clinical parameter or the anatomical location (Table 2A) with histological findings (Table 2B). The results of the different histomorphological methods employed (von Kossa staining, ISL, immunohistochemistry, and *in situ* hybridization) were consistent within the same group (Table 2B). OPG, RANKL, and TRAIL protein and mRNA expression patterns were similar for atherosclerosis and Mönckeberg's sclerosis patients, in that OPG and TRAIL were predominantly adjacent to calcifications and areas of apoptosis throughout the whole circumference of all specimens. Control experi-

TABLE 2. Characteristics of study patients

	Atherosclerosis						Mönckeberg's sclerosis						Control arteries			
	1	2	3	4	5	6	1	2	3	4	5	6	1	2	3	4
A. Clinical parameters																
Age (yr)	78	74	77	68	83	75	83	71	66	60	88	78	57	61	60	49
Sex	F	F	M	M	F	M	F	F	M	M	M	F	M	M	M	F
Stage of vascular insufficiency (stages I–IV)	II	III	II	II	II	IV	IV	IV	IV	II	II	II	0	0	0	0
Vascular region	FA	FA	FA	CA	CA	FA	FA	FA	FA	FA	FA	FA	IMA	IMA	FA	FA
Atherosclerosis risk factors and comorbidity																
Arterial hypertension	+	+	+	+	+	+	+	+	+	+	+	−	+	+	+	−
Hypercholesterolemia	+	−	+	+	+	+	+	+	+	+	−	+	+	+	−	−
Cigarette smoking	−	−	+	+	+	+	−	−	+	−	−	−	−	−	+	−
Diabetes mellitus	−	+	−	−	−	+	+	+	+	−	−	+	−	−	−	−
Chronic renal failure	−	−	−	−	−	−	−	−	−	+	+	+	−	−	−	−
Hypercalcemia	−	−	−	−	−	−	−	−	−	−	−	−	−	−	−	−
B. Histology																
Calcifications																
Intima	+	+	+	+	+	+	−	−	−	+	+	−	−	−	−	−
Media	−	−	−	−	−	−	+	+	+	+	+	+	−	−	−	−
Apoptotic cells																
Intima	+	+	+	+	+	+	−	−	−	+	+	−	−	−	−	−
Media	−	−	−	−	−	−	+	+	+	+	+	+	−	−	−	−
RANKL protein/mRNA expression																
Near calcifications	−/−	−/−	−/−	−/−	−/−	−/−	−/−	−/−	−/−	−/−	−/−	−/−	−/−	−/−	−/−	−/−
Diffuse	+/−	+/−	+/−	+/−	+/−	−/−	+/−	+/−	−/−	+/−	+/−	−/−	−/−	−/−	−/−	−/−
OPG protein/mRNA expression																
Near calcifications	++/++	+/+	++/++	++/++	++/++	++/+	++/++	++/++	++/+	++/++	++/++	+/+	−/−	−/−	−/−	−/−
Diffuse	−/−	−/−	−/−	−/−	−/−	−/−	−/−	−/−	−/−	−/−	−/−	−/−	+/−[a]	+/−[a]	−/−	+/−[a]
TRAIL protein/mRNA expression																
Near calcifications	++/++	++/+	++/++	++/++	++/++	++/+	++/++	++/++	++/+	++/++	++/++	+/+	−/−	−/−	−/−	−/−
Diffuse	−/−	−/−	−/−	−/−	−/−	−/−	−/−	−/−	−/−	−/−	−/−	−/−	−/−	−/−	−/−	−/−

A. Clinical parameters. The mean age was 75.8 yr (range, 68–83 yr) in the atherosclerosis group, 74.3 yr (60–88 yr) in the Mönckeberg's sclerosis group, and 56.7 yr (49–60 yr) in the control group. The stages of vascular insufficiency comprise stages of cerebrovascular insufficiency and peripheral occlusive disease. Stage I is defined as asymptomatic vascular insufficiency. Stage II is characterized by spontaneously reversible ischemic symptoms. Stage III is characterized by prolonged or resting ischemia. Stage IV implies irreversible ischemic damage, such as stroke (cerebro-vascular) or necrosis (peripheral occlusive). The specimens were derived from femoral arteries (FA), carotid arteries (CA), or internal mammary arteries (IMA). Atherosclerosis risk factors and comorbidities defined according to established criteria are indicated. B. Histology. The presence (+) or absence (−) of calcifications demonstrated by von Kossa staining and of apoptotic cells demonstrated by the ISL assay are shown separately for the intimal and medial layers. Protein and mRNA expressions of OPG, RANKL, and TRAIL are demonstrated by immunohistochemistry and *in situ* hybridization, either predominantly near calcifications or diffusely distributed in the intima or media. The staining patterns for protein and mRNA expression are described by the categories no expression (−), moderate expression (+), or strong expression (++).

[a] Endothelial staining.

ments demonstrated that no unspecific binding of DIG to hydroxylapatite occurred (data not shown).

Mönckeberg's sclerosis specimens

Apoptosis was assessed using an ISL to demonstrate DNA fragmentation, a feature of programmed cell death. In Mönckeberg' sclerosis, apoptotic cells (ISL-positive cells) were detected adjacent to calcified plaques and minor calcified lesions in the medial layer, which was composed of smooth muscle cells (Fig. 2F). The number of apoptotic cells in these areas ranged from 2–8.5% (mean, 4%).

OPG and RANKL are crucially involved in bone cell biology by mediating osteoclast functions, and in the animal

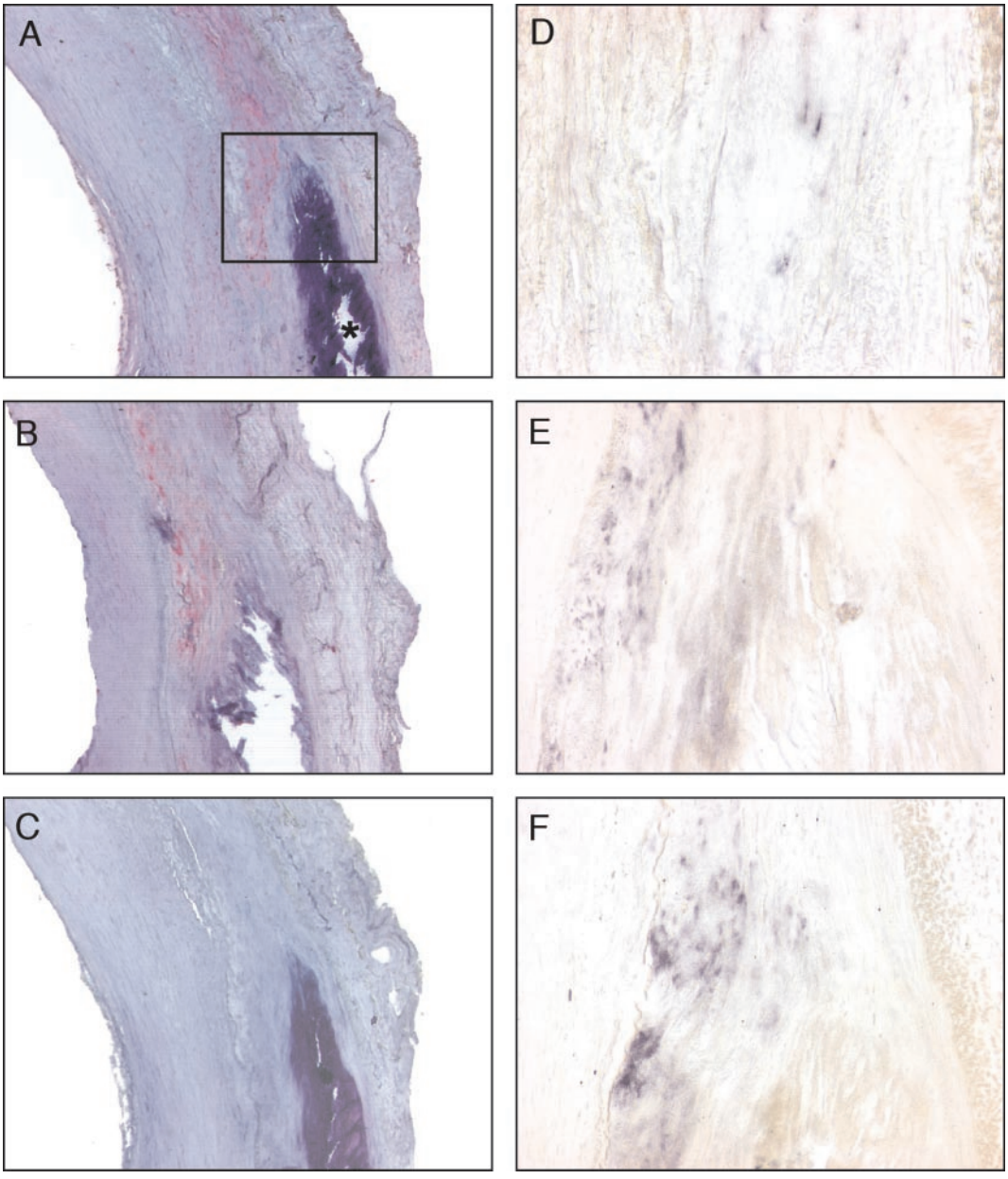

FIG. 2. Serial sections of an artery with medial calcification typical of Mönckeberg's sclerosis without concomitant atherosclerotic neointimal lesions. The *rectangle* in A indicates the respective regions shown in D–F (A–C, 50-fold magnification; D–F, 200-fold magnification). OPG (A) and TRAIL (B) protein expression was demonstrated by immunohistochemistry visualized by streptavidin-alkaline phosphatase conjugate, Fast Red staining (positive reactions are *red*), and Mayer's hemalum counterstaining. The negative control of OPG immunohistochemistry (C) showed the specificity of the reaction by substituting the specific primary antibody with an irrelevant antibody; controls of the other staining procedures were completely negative. OPG and TRAIL were predominantly expressed adjacent to medial calcifications; mRNA production of OPG (D) and TRAIL (E) was demonstrated by *in situ* hybridization visualized by alkaline phosphatase conjugate and NBT/BCIP staining (positive reactions are *dark blue*); there was no counterstaining. Calcifications in A are marked with an *asterisk*. Apoptotic cells were demonstrated in the medial area surrounding calcifications by ISL (F) and visualized by alkaline phosphatase conjugate and NBT/BCIP staining (*dark blue*); there was no counterstaining.

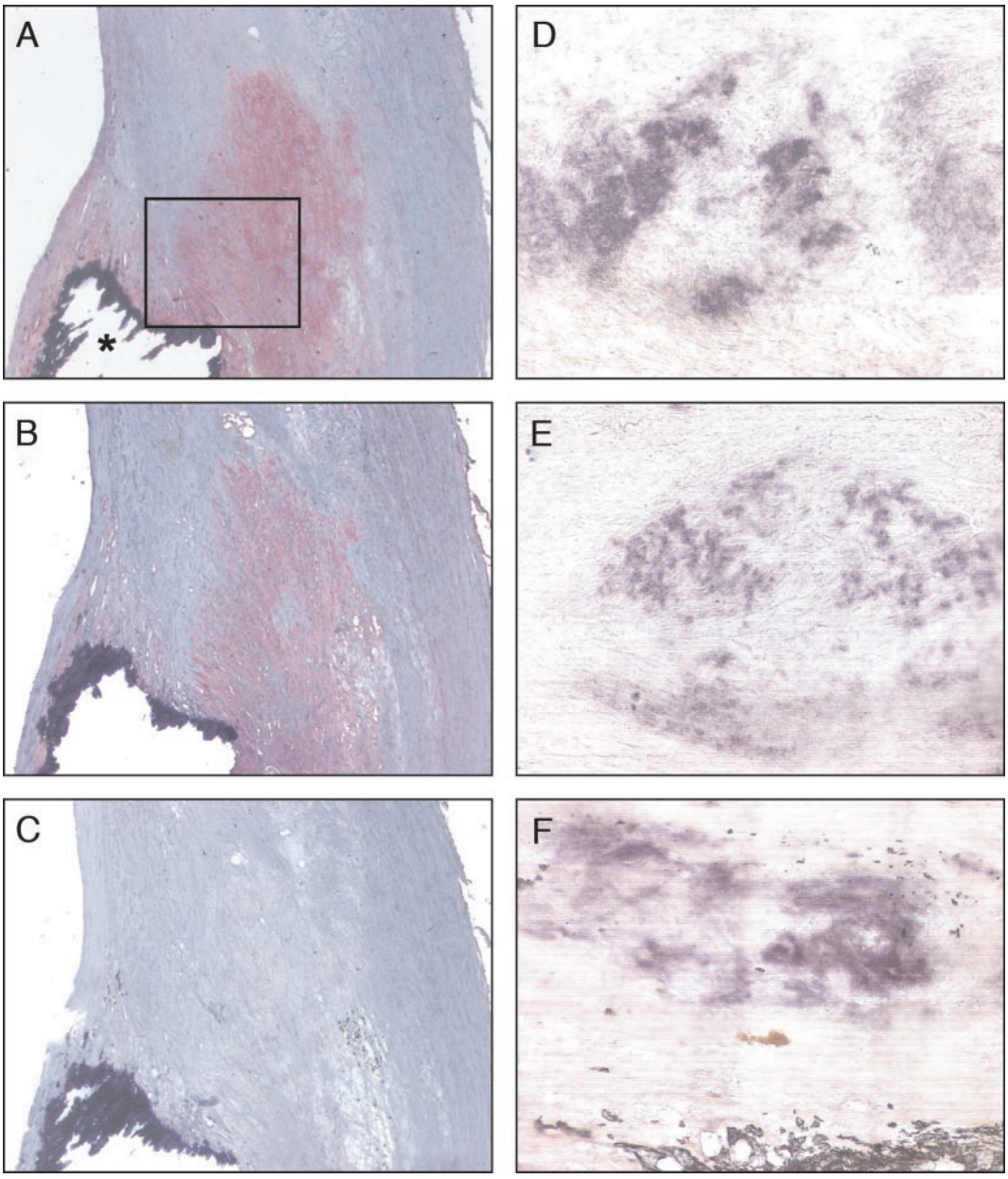

FIG. 3. Serial sections of a typical atherosclerotic specimen with neointimal calcification in the absence of medial calcification, indicated by an *asterisk* (calcified material partly detached). The *rectangle* in A indicates the respective regions shown in D–F (A–C, 50-fold magnification; D–F, 200-fold magnification). OPG (A) and TRAIL (B) immunostaining showed strong expression of both proteins (*red* staining) in the neointimal tissue surrounding calcifications, whereas the negative control of OPG immunohistochemistry (C) demonstrated the specificity of the reaction. OPG (D) and TRAIL (E) mRNA (*dark blue* staining) were detected by *in situ* hybridization. Apoptotic cells (*dark blue* staining) were found in the neointima in the vicinity of calcifications by ISL (F).

model, both cytokines have been detected in the course of vascular calcification (10). OPG immunoreactivity was distributed in the same areas where apoptosis was present, *i.e.* predominantly around calcifications in the media in Mönckeberg's sclerosis (Fig. 2A), whereas RANKL protein was scarcely scattered in these areas (data not shown). The results of OPG immunoreactivity were observed independently by two different monoclonal antibodies directed against OPG (data for clone 69146.11 are not shown).

TRAIL, an inducer of apoptosis in susceptible cells, exhibited a similar spatial staining pattern as OPG in the vicinity of apoptotic areas, suggesting the involvement of TRAIL in the apoptotic processes associated with vascular calcification (Fig. 2B). Of interest, a polyclonal antibody directed against the carboxyl terminus of the TRAIL molecule showed strong staining, whereas a monoclonal antibody directed against biologically active TRAIL showed only weak staining, probably due to TRAIL complexed to antigen (data not shown). Protein detection of OPG and TRAIL was paralleled by mRNA expression of the respective cytokines in Mönckeberg's sclerosis (Fig. 2, D and E), whereas RANKL mRNA could not be detected (data not shown). Thus, OPG

and TRAIL immunoreactivity and mRNA expression showed a similar localization, suggesting that OPG and TRAIL were produced by vessel wall-residing cells.

Atherosclerotic specimens

In contrast to Mönckeberg's sclerosis samples, atherosclerotic specimens exhibited apoptosis mainly in the neointima, with apoptotic cells surrounding foam cell accumulations and calcified lesions (Fig. 3F), and the number of apoptotic cells ranged from 1.5–7% (mean, 3%). As in Mönckeberg's sclerosis, OPG and TRAIL immunoreactivities were distributed predominantly around calcifications in the neointima in atherosclerosis and therefore in the same areas where apoptosis could be detected (Fig. 3, A and B), whereas only faint RANKL staining was seen (data not shown). As before, OPG and TRAIL mRNA were concomitantly detected in the neointima (Fig. 3, D and E), but RANKL mRNA was not found (data not shown).

Normal control specimens

Tissue samples of normal control vessels were ISL negative and did not show apoptosis (Fig. 4F). No immunostaining for TRAIL (Fig. 4B) or RANKL (data not shown) was seen, whereas faint OPG protein expression by endothelial cells

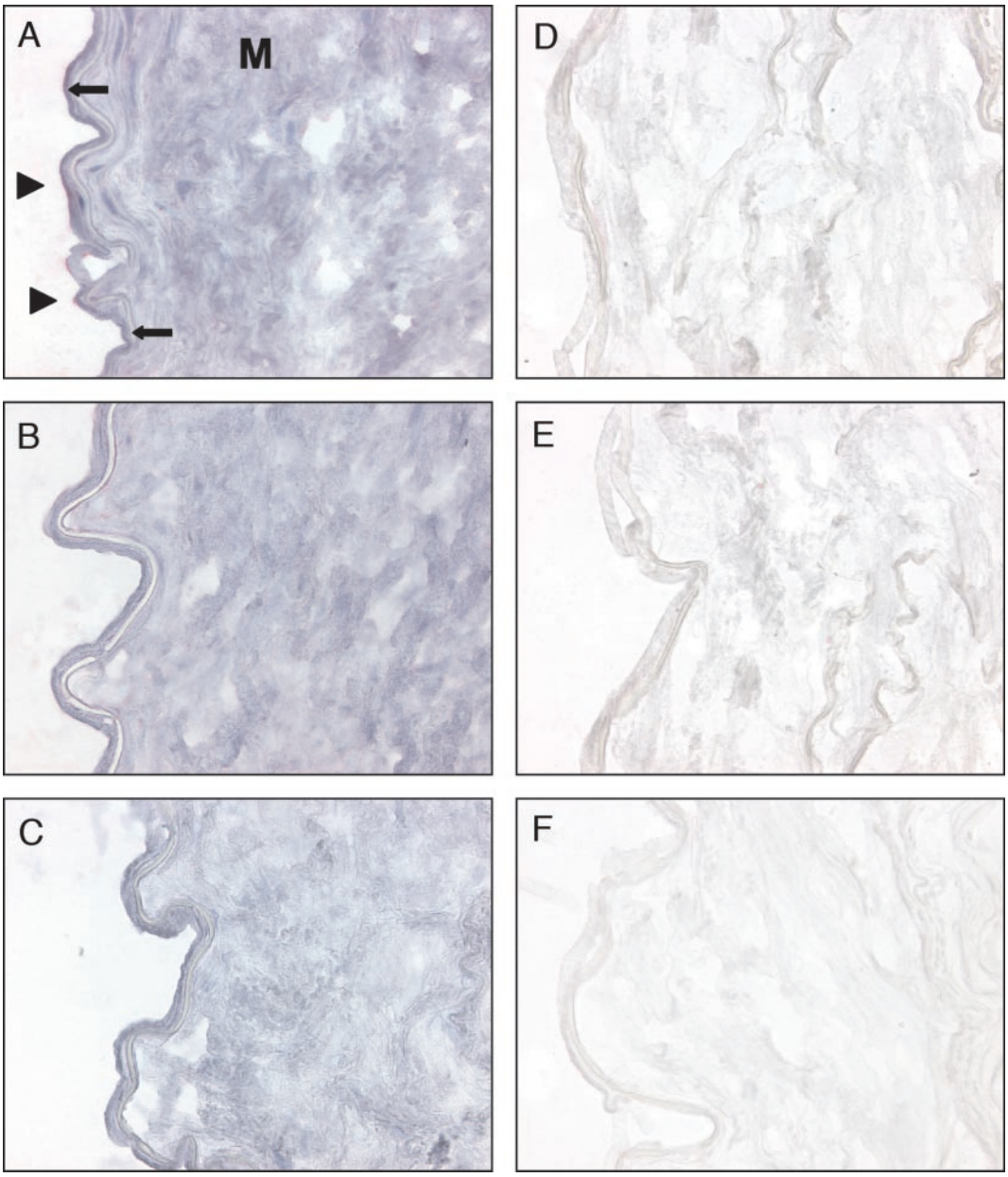

FIG. 4. Serial sections of a normal artery (400-fold magnification) with the intimal, the medial (M), and part of the adventitial layer. Note the thin intimal layer between the lamina elastica interna and the endothelium indicated by *arrows* in A. OPG (A) immunostaining (*arrowheads*) showed faint expression of OPG protein in endothelial cells, whereas OPG mRNA could not be demonstrated (D), possibly due to a low level of mRNA production. TRAIL immunostaining (B) and *in situ* hybridization (E) as well as the immunostaining control (C) and ISL (F) were negative.

was detected (Fig. 4A). However, the low OPG protein expression was not paralleled by OPG mRNA expression (Fig. 4D), and neither TRAIL (Fig. 4E) nor RANKL (data not shown) mRNA was detected. Moreover, there were no differences between normal femoral or internal mammary arteries.

Discussion

Although the precise mechanisms leading to Mönckeberg's sclerosis are largely unknown, apoptotic and osteogenic processes have been hypothesized to contribute to mineralization in Mönckeberg's sclerosis. We have studied specimens from Mönckeberg's sclerosis and atherosclerotic lesions in a small, well characterized cohort of patients and have detected apoptotic processes predominantly adjacent to calcification areas, *i.e.* the media in Mönckeberg's sclerosis and the neointima in atherosclerosis. OPG, a glycoprotein that seems to play a role in the process of vascular calcification in an animal model, and TRAIL, an inducer of apoptosis in susceptible cells, were colocalized to areas of apoptosis.

Targeted deletion of OPG has been shown to result in both osteoporosis and calcifications of the medial layers of the aorta and renal arteries, affecting two thirds of $OPG^{-/-}$ mice (9). A phenotype of medial calcification is also seen in a number of mouse gene knockout studies, such as deficiencies of matrix GLA protein, a vitamin K-dependent circulating and bone-associated protein that can bind calcium in soft tissues (20); SMAD6, an intracellular mediator of bone morphogenetic protein signaling (21); and *Klotho*, a gene associated with aging (22). Furthermore, mice challenged with supraphysiological doses of vitamin D or warfarin treatment exhibit medial calcifications, a phenotype that can be prevented by inhibitors of osteoclasts, including OPG, bisphosphonates, and a selective inhibitor of the osteoclastic $V\text{-}H^{+}$-adenosine triphosphatase, (23–25), providing further evidence for a mechanistic link between vascular calcification and bone metabolism.

Apoptosis has been described to precede calcification *in vitro*, and formation of apoptotic bodies may act as a nucleation site for calcium crystal formation in the vessel wall (1). The detection of TRAIL, a cytokine known to cause apoptosis in a variety of cell lines by ligating one of its several death receptors (8, 26), points to its role in initiating the apoptotic process, yet its role *in vivo* has not been fully elucidated. TRAIL is expressed by vascular smooth muscle cells and may promote cell death in an autocrine or paracrine fashion when induced in conditions such as diabetes, hyperlipidemia, chronic renal failure, or atherosclerosis (27). Of interest, OPG has been described to bind TRAIL and thereby to inhibit its cytotoxic capacity in an *in vitro* model (7). OPG can be detected in the vascular wall (5), and endothelial cells and vascular smooth muscle cells have been reported as its cellular source in the vessel wall (28, 29). The concomitant detection of OPG and TRAIL in apoptotic areas may indicate that increased OPG production at these sites represents a counterregulatory mechanism to limit apoptosis and thereby the initiation of calcification.

OPG and RANKL immunoreactivities in humans have been detected in the normal vascular wall and in early atherosclerotic lesions, whereas in advanced calcified lesions, OPG expression was found in the borders of calcified structures, and RANKL expression was found adjacent to calcium deposits (30). Of note, increased OPG serum levels have been found to be associated with the presence and severity of coronary artery disease (31, 32), which may indicate an insufficient counterregulatory mechanism in light of the protective role of OPG in the vascular system. However, a recent study suggests that OPG and matrix GLA protein may be down-regulated in calcified arteries (33), whereas the expression of transcription factors that regulate mineralization and osseous differentiation programs (34) and the up-regulation of osteogenic genes, such as alkaline phosphatase, bone sialoprotein, or bone GLA protein, in vascular smooth muscle cells in the course of medial calcification has been demonstrated (14). Of interest, dexamethasone enhances differentiation of vascular smooth muscle cells toward an osteoblastic phenotype *in vitro* (35) and concurrently inhibits OPG expression by osteoblasts (36).

In summary, we have found apoptosis around calcified regions of Mönckeberg's sclerosis and atherosclerotic arteries, with the concurrent detection of OPG and TRAIL in these areas. Apoptotic cells may serve as a matrix for calcification, with TRAIL-induced apoptosis being an initiator of this process (Fig. 5). The OPG/RANKL system has been shown to regulate mineralization processes, and OPG may act as a potential counterregulatory and antiapoptotic factor. Further work is necessary to elucidate the exact mechanisms that lead to vascular calcification to develop preventive strategies.

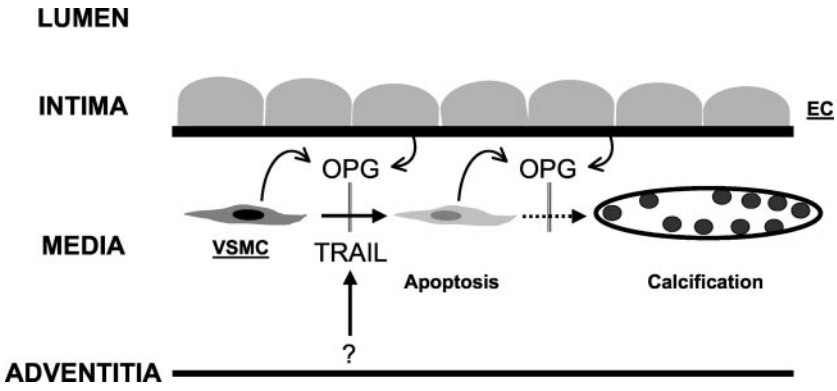

FIG. 5. Hypothetical model illustrating the potential mechanisms of the OPG system involved in the process of vascular calcification in Mönckeberg's sclerosis. Under pathological conditions (*i.e.* the presence of cardiovascular risk factors), TRAIL expression is upregulated and may cause the initiation of apoptosis in susceptible cells, such as vascular smooth muscle cells. The formation of apoptotic bodies serves as a substrate for calcium crystal deposition in the medial layer of the vascular wall. OPG, which is produced by endothelial cells and vascular smooth muscle cells, acts as a decoy receptor for TRAIL to prevent apoptosis and, in addition, may prevent vascular calcification through as yet unidentified mechanisms.

Acknowledgments

We thank Olga Dakischew for her experienced technical assistance.

Received August 18, 2003. Accepted May 14, 2004.

Address all correspondence and requests for reprints to: Dr. Michael Schoppet, Department of Internal Medicine and Cardiology, Philipps University, Baldingerstrasse, D-35033 Marburg, Germany. E-mail: schoppet@mailer.uni-marburg.de.

This work was supported by a Heisenberg fellowship from the Deutsche Forschungsgemeinschaft (to L.C.H.; Ho 1875/3-1 and Ho 1875/4-1).

M.S. and N.A.-F. contributed equally to this work.

References

1. **Proudfoot D, Skepper JN, Hegyi L, Bennett MR, Shanahan CM, Weissberg PL** 2000 Apoptosis regulates human vascular calcification in vitro: evidence for initiation of vascular calcification by apoptotic bodies. Circ Res 87:1055–1062
2. **Ross R** 1999 Atherosclerosis: an inflammatory disease. N Engl J Med 340:115–126
3. **Amos RS, Wright V** 1980 Monckeberg's arteriosclerosis and metabolic bone disease. Lancet 2:248–249
4. **Lehto S, Niskanen L, Suhonen M, Ronnemaa T, Laakso M** 1996 Medial artery calcification. A neglected harbinger of cardiovascular complications in non-insulin-dependent diabetes mellitus. Arterioscler Thromb Vasc Biol 16:978–983
5. **Simonet WS, Lacey DL, Dunstan CR, Kelley M, Chang MS, Luthy R, Nguyen HQ, Wooden S, Bennett L, Boone T, Shimamoto G, DeRose M, Elliott R, Colombero A, Tan HL, Trail G, Sullivan J, Davy E, Bucay N, Renshaw-Gegg L, Hughes TM, Hill D, Pattison W, Campbell P, Sander S, Van G, Tarpley J, Derby P, Lee R, Amgen EST Program, Boyle WJ** 1997 Osteoprotegerin: a novel secreted protein involved in the regulation of bone density. Cell 89:309–319
6. **Hsu H, Lacey DL, Dunstan CR, Solovyev I, Colombero A, Timms E, Tan HL, Elliott G, Kelley MJ, Sarosi I, Wang L, Xia XZ, Elliott R, Chiu L, Black T, Scully S, Capparelli C, Morony S, Shimamoto G, Bass MB, Boyle WJ** 1999 Tumor necrosis factor receptor family member RANK mediates osteoclast differentiation and activation induced by osteoprotegerin ligand. Proc Natl Acad Sci USA 96:3540–3545
7. **Emery JG, McDonnell P, Burke MB, Deen KC, Lyn S, Silverman C, Dul E, Appelbaum ER, Eichman C, DiPrinzio R, Dodds RA, James IE, Rosenberg M, Lee JC, Young PR** 1998 Osteoprotegerin is a receptor for the cytotoxic ligand TRAIL. J Biol Chem 273:14363–14367
8. **Degli-Esposti M** 1999 To die or not to die: the quest of the TRAIL receptors. J Leukoc Biol 65:535–542
9. **Bucay N, Sarosi I, Dunstan CR, Morony S, Tarpley J, Capparelli C, Scully S, Tan HL, Xu W, Lacey DL, Boyle WJ, Simonet WS** 1998 Osteoprotegerin-deficient mice develop early onset osteoporosis and arterial calcification. Genes Dev 12:1260–1268
10. **Min H, Morony S, Sarosi I, Dunstan CR, Capparelli C, Scully S, Van G, Kaufman S, Kostenuik PJ, Lacey DL, Boyle WJ, Simonet WS** 2000 Osteoprotegerin reverses osteoporosis by inhibiting endosteal osteoclasts and prevents vascular calcification by blocking a process resembling osteoclastogenesis. J Exp Med 192:463–474
11. **Mönckeberg JG** 1902 Über die reine Mediaverkalkung der Extremitätenarterien und ihr Verhalten zur Arteriosklerose. Virchows Arch Pathol Anat 171:141–167
12. **Silver MD, Gotlieb AI, Schoen FJ, eds** 2001 Cardiovascular pathology, 3rd ed. New York, London: Churchill Livingstone; 68–106
13. **Stary HC, Chandler AB, Dinsmore RE, Fuster V, Glagov S, Insull W, Rosenfeld ME, Schwartz CJ, Wagner WD, Wissler RW** 1995 A definition of advanced types of atherosclerotic lesions and a histological classification of atherosclerosis. A report from the Committee on Vascular Lesions of the Council on Arteriosclerosis, American Heart Association. Circulation 92:1355–1374
14. **Shanahan CM, Cary NRB, Salisbury JR, Proudfoot D, Weissberg PL, Edmonds ME** 1999 Medial localization of mineralization-regulating proteins in association with Mönckeberg's sclerosis: evidence for smooth muscle cell-mediated vascular calcification. Circulation 100:2168–2176
15. **Didenko VV, Hornsby PJ** 1996 Presence of double-strand breaks with single-base 3′ overhangs in cells undergoing apoptosis but not necrosis. J Cell Biol 135:1369–1376
16. **Al-Fakhri N, Chavakis T, Schmidt-Woll T, Huang B, Cherian SM, Bobryshev YV, Lord RSA, Katz N, Preissner KT** 2003 Induction of apoptosis in vascular cells by plasminogen activator inhibitor-1 and high molecular weight kininogen correlates with their anti-adhesive properties. J Biol Chem 384:423–435
17. **Chomczynski P, Sacchi N** 1987 Single-step method of RNA isolation by acid guanidinium thiocyanate-phenol-chloroform extraction. Anal Biochem 162:156–159
18. **Hanaki K, Nakatake H, Yamamoto K, Odawara T, Yoshikura H** 2000 DNase I activity retained after heat inactivation in standard buffer. BioTechniques 29:38–42
19. **Wiame I, Remy S, Swennen R, Sagi L** 2000 Irreversible heat inactivation of DNase I without RNA degradation. BioTechniques 29:252–256
20. **Luo G, Ducy P, McKee MD, Pinero GJ, Loyer E, Behringer RR, Karsenty G** 1997 Spontaneous calcification of arteries and cartilage in mice lacking matrix GLA protein. Nature 386:78–81
21. **Galvin KM, Donovan MJ, Lynch CA, Meyer RI, Paul RJ, Lorenz JN, Fairchild-Huntress V, Dixon KL, Dunmore JH, Gimbrone MA, Falb D, Huszar D** 2000 A role for SMAD6 in development and homeostasis of the cardiovascular system. Nat Genet 24:171–174
22. **Kuro-o OM, Matsumura Y, Aizawa H, Kawaguchi H, Suga T, Utsugi T, Ohyama Y, Kurabayashi M, Kaname T, Kume E, Iwasaki H, Iida A, Shiraki-Iida T, Nishikawa S, Nagai R, Nabeshima YI** 1997 Mutation of the mouse klotho gene leads to a syndrome resembling aging. Nature 390:45–51
23. **Price PA, June HH, Buckley JR, Williamson MK** 2001 Osteoprotegerin inhibits artery calcification induced by warfarin and by vitamin D. Arterioscler Thromb Vasc Biol 21:1610–1616
24. **Price PA, Faus SA, Williamson MK** 2001 Bisphosphonates alendronate and ibandronate inhibit artery calcification at doses comparable to those that inhibit bone resorption. Arterioscler Thromb Vasc Biol 21:817–824
25. **Price PA, June HH, Buckley JR, Williamson MK** 2002 SB 242784, a selective inhibitor of the osteoclastic V-H^+-ATPase, inhibits arterial calcification in the rat. Circ Res 91:547–552
26. **Wiley SR, Schooley K, Smolak PJ, Din WS, Hunag CP, Nicholl JK, Sutherland GR, Smith TD, Rauch C, Smith CA, Goodwin RG** 1995 Identification and characterization of a new member of the TNF family that induces apoptosis. Immunity 3:673–682
27. **Gochuico BR, Zhang J, Ma BY, Marshak-Rothstein A, Fine A** 2000 TRAIL expression in vascular smooth muscle. Am J Physiol 278:L1045–L1050
28. **Collin-Osdoby P, Rothe L, Anderson F, Nelson M, Maloney W, Osdoby P** 2001 Receptor activator of NF-κB and osteoprotegerin expression by human microvascular endothelial cells, regulation by inflammatory cytokines, and role in human osteoclastogenesis. J Biol Chem 276:20659–20672
29. **Zhang J, Fu M, Myles D, Zhu X, Du J, Cao X, Chen YE** 2002 PDGF induces osteoprotegerin expression in vascular smooth muscle cells by multiple signal pathways. FEBS Lett 521:180–184
30. **Dhore CR, Cleutjens JP, Lutgens E, Cleutjens KB, Geusens PP, Kitslaar PJ, Tordoir JH, Spronk HM, Vermeer C, Daemen MJ** 2001 Differential expression of bone matrix regulatory proteins in human atherosclerotic plaques. Arterioscler Thromb Vasc Biol 21:1998–2003
31. **Jono S, Ikari Y, Shioi A, Mori K, Miki T, Hara K, Nishizawa Y** 2002 Serum osteoprotegerin levels are associated with the presence and severity of coronary artery disease. Circulation 106:1192–1194
32. **Schoppet M, Sattler AM, Schaefer JR, Herzum M, Maisch B, Hofbauer LC** 2003 Increased osteoprotegerin serum levels in men with coronary artery disease. J Clin Endocrinol Metab 88:1024–1028
33. **Tyson KL, Reynolds JL, McNair R, Zhang Q, Weissberg PL, Shanahan CM** 2003 Osteo/chondrocytic transcription factors and their target genes exhibit distinct patterns of expression in human arterial calcification. Arterioscler Thromb Vasc Biol 23:489–494
34. **Towler DA, Bidder M, Latifi T, Coleman T, Semenkovich CF** 1998 Diet-induced diabetes activates an osteogenic gene regulatory program in the aortas of low density lipoprotein receptor-deficient mice. J Biol Chem 273:30427–30434
35. **Mori K, Shioi A, Jono S, Nishizawa Y, Morii H** 1999 Dexamethasone enhances in vitro vascular calcification by promoting osteoblastic differentiation of vascular smooth muscle cells. Arterioscler Thromb Vasc Biol 19:2112–2118
36. **Hofbauer LC, Gori F, Riggs BL, Lacey DL, Dunstan CR, Spelsberg TC, Khosla S** 1999 Stimulation of osteoprotegerin ligand and inhibition of osteoprotegerin production by glucocorticoids in human osteoblastic lineage cells: potential paracrine mechanisms of glucocorticoid-induced osteoporosis. Endocrinology 140:4382–4389